Pure qP-wave propagation in VTI media

Jörg Schleicher (IMECC/UNICAMP & INCT-GP), and Jessé C. Costa (FGeo/UFPA & INCT-GP)

Abstract

The qP and qS-wave eikonal equations derived from the VTI wave equation show that in the pseudo-acoustic approximation, their dispersion relations degenerate into a single one. Therefore, when using this dispersion relation for wave simulation, for instance by means of finite-difference approximations, both events are generated. To avoid the occurrence of the pseudo-S wave, the qP-wave dispersion relation alone needs to be approximated. This can be done with or without the pseudo-acoustic approximation. A Padé approximation with slightly unconventional numbers for the Padé coefficients led to the best approximation. An implementation of a low-rank approximation to this equation demonstrates that this can provide high-accuracy wavefields even in strongly anisotropic inhomogeneous media.

Introduction

Reverse time migration using anisotropic velocity models has become the standard methodology for seismic imaging in complex exploration settings. Although anisotropy is essentially an elastic property, migration with elastic wave equation is currently unfeasible. Even if one is able to successfully estimate elastic migration velocity models, the computational cost to solve elastic wave equation and the lack of efficient algorithms to compute wave mode separation are major obstacles to elastic imaging. In this scenario, pseudo-acoustic approximation (Alkhalifah, 1998, 2000) is a very cost-effective approach to anisotropic RTM. The pseudo-acoustic wave equation, proposed to model the evolution of qP modes, is derived under the assumption that shear velocity is zero along the symmetry axis.

However, finite difference implementations of pseudo-acoustic wave equation can be plagued by physical instability and undesirable S-wave modes even in the weakly anisotropic regime. Several strategies have been proposed to overcome these problems. Stability of space-time FD implementations of the pseudo-acoustic wave equation can be only be assured if the Thomsen parameters satisfy the constraint $\varepsilon \geq \delta$, which is not always valid for shales (Thomsen, 1986). Fletcher et al. (2009) and Fowler et al. (2010) showed that a stable approximation for qP modes in VTI media can be derived if one does not assume the shear velocity along the symmetry axis to be zero. However, their proposed stable coupled system of second-order differential equations still can produce undesirable S-wave modes.

The mitigation of the S-wave in FD implementations of the pseudo-acoustic approximation has been an area of active research since the original work of Alkhalifah (1998). For example, Alkhalifah (2003) indicated that if the source is in an isotropic region the S modes are not generated, although it still can be produced at interfaces with sharp contrast. The work of Grechka et al. (2004) indicates that the instability of pseudo-acoustic wave-equation is due to the coupling of the S mode to the qP mode. The S mode is not stable when $\varepsilon \geq \delta$.

For this reason, one solution to obtain a stable qP wave equation is to factor out these spurious modes from the pseudo-acoustic wave equation. The work of Klíe and Toro (2001) presents one such approximation for pure qP wave-equation under the assumption of weak anisotropy. Exact factorization results in a pseudo-differential operator in the mixed space-wavenumber domain (Liu et al., 2009). Differential equations in space-time for the pure qP mode can be derived through approximations to the exact pseudo-differential operator for qP evolution. Liu et al. (2009) proposed an algorithm to implement the exact factorization of the pseudo-acoustic wave equation in the mixed space-wavenumber domain. Pestana et al. (2012) derive an alternative approximation for the exact factorization which is valid for weak anisotropy and can be implemented using finite difference in time and pseudo-spectral method in space. More sophisticated approximations of this factorization can be found in Du et al. (2014). Most recently, the exact factorization of the pseudo-acoustic wave equation in the mixed space-wavenumber domain has been implemented using the low-rank approximation (Sergey Fomel et al., 2013; Song and Alkhalifah, 2013; Wu and Alkhalifah, 2014).

In this work, we derive a new pure qP-mode approximation free of physical instability and S modes and valid even for strong anisotropic media. Numerical experiments in strong anisotropic media with positive and negative anellipticity indicate the accuracy and stability of the implementation and demonstrate that the S modes are eliminated from the proposed qP equation for weak and strong anisotropic models. We also present simulations in a smoothly heterogeneous medium.

Theory

Elastic wave propagation in a VTI medium

We start at the approximate elastic wave equation for VTI media with small δ, as specified by Bloot et al. (2013). Still according to Bloot et al. (2013), substitution of a zero-order ray ansatz (Červený, 1985; Červený, V., 2001) with $\mathbf{U}$ denoting a vectorial amplitude and T denoting the

traveltime, into the VTI wave equation without a source term yields the eigenvalue problem

$$\underline{\Gamma}\mathbf{U} = \mathbf{U}, \tag{1}$$

where the eigenvalues are all $\Lambda = 1$. The Christoffel matrix $\underline{\Gamma}$ has the elements

$$\begin{aligned}
\Gamma_{11} &= (\alpha^2-\beta^2)p_1^2+\beta^2\|\mathbf{p}\|^2+2\varepsilon\alpha^2p_1^2+2\gamma\beta^2p_2^2,\\
\Gamma_{22} &= (\alpha^2-\beta^2)p_2^2+\beta^2\|\mathbf{p}\|^2+2\varepsilon\alpha^2p_2^2+2\gamma\beta^2p_1^2,\\
\Gamma_{33} &= (\alpha^2-\beta^2)p_3^2+\beta^2\|\mathbf{p}\|^2,\\
\Gamma_{21} &= \Gamma_{12} = (\alpha^2-\beta^2)p_1p_2+2(\varepsilon\alpha^2-\gamma\beta^2)p_1p_2,\\
\Gamma_{31} &= \Gamma_{13} = (\alpha^2-\beta^2)p_1p_3+\delta\alpha^2p_1p_3,\\
\Gamma_{32} &= \Gamma_{23} = (\alpha^2-\beta^2)p_2p_3+\delta\alpha^2p_2p_3.
\end{aligned} \tag{2}$$

where the slowness vector $\mathbf{p}$ is defined as

$$\mathbf{p} = \nabla T = (p_1, p_2, p_3)\ . \tag{3}$$

Moreover,

$$\alpha = \sqrt{\frac{\lambda+2\mu}{\rho}} \qquad \text{and} \qquad \beta = \sqrt{\frac{\mu}{\rho}} \tag{4}$$

denote the vertical P and S wave velocities, and ε and δ are the Thomsen parameters.

Bloot et al. (2013) calculated three eigenvalues Λ of $\underline{\Gamma}$ exactly to obtain

$$\Lambda_{1,2} = \frac{1}{2}\left((\alpha^2+\beta^2)\|\mathbf{p}\|^2+2\varepsilon\alpha^2\|\widehat{\mathbf{p}}\|^2 \pm \sqrt{(\alpha^2-\beta^2)^2\|\mathbf{p}\|^4+4\Pi}\right) \tag{5}$$

and

$$\Lambda_3 = \beta^2\|\mathbf{p}\|^2+2\gamma\beta^2\|\widehat{\mathbf{p}}\|^2, \tag{6}$$

where the horizontal slowness vector $\widehat{\mathbf{p}}$ is given by

$$\widehat{\mathbf{p}} = \widehat{\nabla} T = (p_1, p_2, 0)\ , \tag{7}$$

and where, up to first order in δ,

$$\Pi = \alpha^2\left[(\alpha^2-\beta^2)\left(\varepsilon\|\mathbf{p}\|^2+2(\delta-\varepsilon)p_3^2\right)+\alpha^2\varepsilon^2\|\widehat{\mathbf{p}}\|^2\right]\|\widehat{\mathbf{p}}\|^2. \tag{8}$$

The condition that the eigenvalues must be equal to one in order to correspond to a solution to equation (1) translates thus into

$$\Lambda_{1,2} = A_+ \pm \sqrt{A_-^2 - B} = 1 \tag{9}$$

and

$$\Lambda_3 = C = 1 \tag{10}$$

where

$$A_\pm = \frac{1}{2}\left((\alpha^2\pm\beta^2)\|\mathbf{p}\|^2+2\varepsilon\alpha^2\|\widehat{\mathbf{p}}\|^2\right) \tag{11}$$

$$B = 2\alpha^2(\alpha^2-\beta^2)(\varepsilon-\delta)p_3^2\|\widehat{\mathbf{p}}\|^2 \tag{12}$$

$$C = \beta^2\left(\|\mathbf{p}\|^2+2\gamma\|\widehat{\mathbf{p}}\|^2\right) \tag{13}$$

If higher orders in δ are taken into account, a term $\alpha^4p_3^2\|\widehat{\mathbf{p}}\|^2\delta^2$ must be subtracted from B in equation (12).

Equation (9) with a positive sign is the qP eikonal equation that describes the kinematic properties of qP-wave propagation, and with a negative sign it is the qSV eikonal equation. Correspondingly, equation (10) is the qSH eikonal equation.

Pseudo-acoustic approximation

The pseudo-acoustic approximation (Alkhalifah, 1998, 2000) consists of setting the vertical S-wave velocity to zero in the equations governing wave propagation. With $\beta = 0$, equations (9) and (10) become

$$\Lambda_{1,2} = a \pm \sqrt{a^2-b} = 1\ , \tag{14}$$

$$\Lambda_3 = 0\ , \tag{15}$$

where now

$$a = \frac{\alpha^2}{2}\left(\|\mathbf{p}\|^2+2\varepsilon\|\widehat{\mathbf{p}}\|^2\right)\ , \tag{16}$$

$$b = 2\alpha^4(\varepsilon-\delta)p_3^2\|\widehat{\mathbf{p}}\|^2\ . \tag{17}$$

For higher orders in δ, again the term $\alpha^4p_3^2\|\widehat{\mathbf{p}}\|^2\delta^2$ must be subtracted from b in equation (17).

Equation (15) implies that qSH-wave propagation in impossible in a pseudo-acoustic VTI medium. At first view, the situation of qP and qSV-wave propagation is less clear. A simple analysis of equation (14) reveals that it can be rewritten as

$$\begin{aligned}
\pm\sqrt{a^2-b} &= 1-a\\
a^2-b &= 1-2a+a^2\\
\text{or}\qquad 2a-b &= 1\ .
\end{aligned} \tag{18}$$

Replacing $\|\widehat{\mathbf{p}}\|^2 \to \frac{k_x^2}{\omega^2}$, $p_3^2 \to \frac{k_z^2}{\omega^2}$, $\alpha^2 \to \frac{v_n^2}{1+2\delta}$, $\frac{\varepsilon-\delta}{1+2\delta} \to \eta$, where k_x and k_z denote the horizontal and vertical wavenumbers and v_n is the NMO velocity, we arrive at

$$k_z^2 = \frac{v_n^2}{\alpha^2}\left(\frac{\omega^2}{v_n^2}-\frac{\omega^2k_x^2}{\omega^2-2\eta v_n^2k_x^2}\right)\ , \tag{19}$$

which is exactly the pseudo-acoustic qP dispersion relation of Alkhalifah (2000). Since in the analysis leading to equation (18), we have taken into account both signs in front of the square root, this equation is actually a dispersion relation for both, qP and qSV waves.

Pseudo-acoustic qP and qSV degeneration

Pseudo-acoustic qP and qSV waves degenerate into a single arrival, if

$$\pm\sqrt{a^2-b} = 1-a = 0\ . \tag{20}$$

Equation (20) immediately implies that $a = b = 1$, i.e.,

$$a = \frac{\alpha^2}{2}\left((1+2\varepsilon)\|\widehat{\mathbf{p}}\|^2+p_3^2\right) = 1\ , \tag{21}$$

$$b = 2\alpha^4(\varepsilon-\delta)p_3^2\|\widehat{\mathbf{p}}\|^2 = 1\ . \tag{22}$$

These two equations define the propagation directions in which pseudo-acoustic qP and qSV waves travel with the same velocity. Solving equation (21) for p_3^2 and substituting the resulting expression in equation (22) results in

$$(1+2\varepsilon)\alpha^4\|\widehat{\mathbf{p}}\|^4-2\alpha^2\|\widehat{\mathbf{p}}\|^2+1/(2\varepsilon-2\delta) = 0\ , \tag{23}$$

which can be solved for the horizontal slowness to yield

$$\|\widehat{\mathbf{p}}\|^2 = \frac{1}{\alpha^2}\frac{1\pm\sqrt{-\frac{1+2\delta}{2(\varepsilon-\delta)}}}{1+2\varepsilon}\ . \tag{24}$$

Note, however, that equations (21) and (22) cannot be satisfied simultaneously for an arbitrary VTI medium. For equation (22) to be fulfilled, we need $\varepsilon - \delta > 0$. For equation (24) to represent a real propagation direction, i.e., describing a nonevanescent wave, the term under the square root must be nonnegative. This condition translates to the requirement that $\varepsilon - \delta < 0$, unless $\delta = -1/2$. Thus, as already observed by Grechka et al. (2004), qP-qSV wave degeneration is possible only in media with $\delta = -1/2$. Note that the same analysis carried out up to second order in δ yields for this condition $\delta = 1 - \sqrt{2} \approx -0.41$, allowing this degeneration to occur in more realistic media.

In a medium satisfying this condition, equation (24) reduces to

$$\alpha^2 \|\widehat{\mathbf{p}}\|^2 = \frac{1}{1+2\varepsilon} \ . \tag{25}$$

The vertical slowness component is then given by substituting equation (25) into equation (21), which yields

$$\alpha^2 p_3^2 = 2 - (1+2\varepsilon)\alpha^2 \|\widehat{\mathbf{p}}\|^2 = 1 \ . \tag{26}$$

Equations (25) and (26) correspond to the propagation direction (see again Grechka et al., 2004)

$$\theta = \arctan \frac{p_1}{p_3} = \pm \arctan \frac{1}{\sqrt{1+2\varepsilon}} = \pm \frac{1}{2} \arccos \frac{1}{1+\varepsilon} \ . \tag{27}$$

Separate pseudo-acoustic qP and qSV propagation

From the above analysis, it is clear that to propagate qP waves or qSV waves only, we must not rely on the common dispersion relation (19). The individual eikonal equations

$$\text{qP eikonal equation:} \quad + \sqrt{a^2 - b} = 1 - a \tag{28}$$

$$\text{qSV eikonal equation:} \quad - \sqrt{a^2 - b} = 1 - a \tag{29}$$

must be considered.

The positive sign in front of the square root in the qP eikonal equation (28) shows that this equation can only be fulfilled if $1 - a > 0$, i.e., $a < 1$. Moreover, since we are interest in describing transient waves, we need the argument of the square-root to be positive, which translates into the condition $b < a^2$. Correspondingly, we see that the qSV eikonal equation (29) requires $a > 1$ and $b < a^2$. Moreover, equation (29) cannot be fulfilled if $b < 0$, because in that case the left-hand side $-\sqrt{a^2 - b} < -a$, while the right-hand side $1 - a > -a$. Thus, for transient pseudo-acoustic qSV-wave propagation to be possible, we need $0 < b < a^2$. The condition $b > 0$ directly implies $\varepsilon - \delta > 0$. Thus, the pseudo-acoustic qSV wave can only be observed in VTI media with $\varepsilon > \delta$, i.e., $\eta > 0$.

This analysis demonstrates that the domains for qP and qSV waves are separated by the surface $a = 1$, which is an elliptical slowness surface with horizontal velocity $\alpha\sqrt{(1+2\varepsilon)/2}$ and vertical velocity $\alpha\sqrt{1/2}$.

Approximations to the pseudo-acoustic qP eikonal equation

Because we are interested in describing the propagation of qP waves only, we need to transform equation (28) into a differential equation, which can then be solved, e.g., by means of a finite-difference approximation. However, since equation (28) contains a square root, it cannot be used directly to derive an equivalent wave equation. Therefore, we study a few possible approximations to the square root.

Near vertical propagation

The first idea is to approximate square root for near-vertical propagation, i.e., for $\|\widehat{\mathbf{p}}\|^2 \ll p_3^2$. Writing the square root in equation (28) in terms of $\|\widehat{\mathbf{p}}\|^2 / p_3^2$, we find up to first order

$$\sqrt{\left(\frac{\alpha^2}{2}(\|\mathbf{p}\|^2 + 2\varepsilon\|\widehat{\mathbf{p}}\|^2)\right)^2 - 2\alpha^4(\varepsilon-\delta)p_3^2\|\widehat{\mathbf{p}}\|^2}$$
$$\approx \frac{\alpha^2}{2}\left((1-2\varepsilon+4\delta)\|\widehat{\mathbf{p}}\|^2 + p_3^2\right) \qquad (\|\widehat{\mathbf{p}}\|^2 \ll p_3^2) \ . \tag{30}$$

Substitution back in equation (28) yields an approximate elliptical eikonal equation

$$v_n^2 \|\widehat{\mathbf{p}}\|^2 + \alpha^2 p_3^2 = 1 \ . \tag{31}$$

Alternative approximation

Another promising idea is to approximate square root for $b \ll a^2$, given that it has to satisfy $b < a^2$ anyway for the square root to remain real. We find

$$\begin{aligned} \sqrt{a^2 - b} &= a\sqrt{1 - \frac{b}{a^2}} \approx a\left(1 - \frac{b}{2a^2}\right) \\ &= a - \frac{b}{2a} \qquad (b \ll a^2) \end{aligned} \tag{32}$$

This leads to the approximate eikonal equation

$$a - \frac{b}{2a} \approx 1 - a \tag{33}$$

$$\text{or} \qquad 2a(2a-1) = b \ . \tag{34}$$

The corresponding dispersion relation has been previously derived, transformed into a differential equation and numerically tested through an FD implementation by Klíe and Toro (2001).

Non-acoustic qP eikonal equation

The structure of the original eikonal equations (9) is almost identical to its pseudo-acoustic version (14). Therefore, the same approximation that lead to Klíe and Toro's equation above can also be directly applied to the former. For $B \ll A_-^2$, we find the approximate square root

$$\sqrt{A_-^2 - B} \approx A_- - \frac{B}{2A_-} \ , \tag{35}$$

which leads to the approximate eikonal equation

$$A_+ + A_- - \frac{B}{2A_-} \approx 1 \ , \tag{36}$$

or, with $A_+ + A_- = 2a$ (compare equations (11) and (16)),

$$2A_-(2a-1) = B \ . \tag{37}$$

The corresponding dispersion relation has been derived in a different way by Pestana et al. (2012), based on a factorization of the dispersion relation by Du et al. (2008).

Equation (37) has some properties that are worthwhile to note: It

- Reduces to Klíe and Toro's equation for $\beta = 0$;
- Allows stable implementation for $\eta < 0$;
- Possesses only a weak dependence on β.

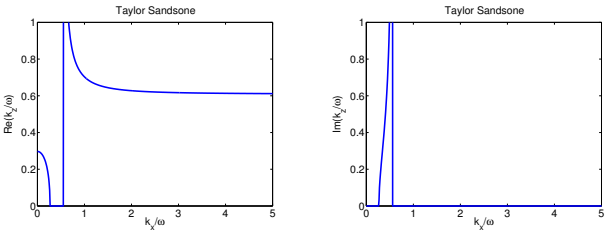

Real part Imaginary part

Figure 1: Pseudo-acoustic qP dispersion relation for Taylor Sandstone. The dispersion relation becomes imaginary at the horizontal P-wave velocity, but turns real again for larger k_x.

The latter observation is important because it means that the approximation can be expected to work even if using a constant ratio between the vertical P and S-wave velocities, which helps to reduce the number of required parameters to the same number used in the equation of Klíe and Toro (2001).

Strong-anisotropy approximation

For values of B close to A_-^2, this approximation may not have sufficient quality. A better approximation of the square root can be achieved by means of a fractional Padé approximation, i.e.,

$$A_- \sqrt{1 - \frac{B}{A_-^2}} \approx A_- \left(1 - \frac{q_1 \frac{B}{A_-^2}}{1 - q_2 \frac{B}{A_-^2}} \right) , \qquad (38)$$

where q_1 and q_2 are the Padé coefficients. The corresponding approximate eikonal equation reads

$$A_+ + A_- - \frac{q_1 \frac{B}{A_-}}{1 - q_2 \frac{B}{A_-^2}} \approx 1 \qquad (39)$$

or, equivalently,

$$(A_-^2 - q_2 B)(2a - 1) = q_1 A_- B \, . \qquad (40)$$

Numerical Examples

To better understand the S-wave modes in the pseudo-acoustic approximation and to demonstrated the quality of the approximations obtained from the above analysis, we have calculated a number of slowness surfaces and modeled wave propagation for a set of differently anisotropic media.

Pseudo-acoustic qP dispersion relation

The S-wave modes in the pseudo-acoustic approximation are best understood from an analysis of the pseudo-acoustic qP dispersion relation. Figure 1 shows this relation for the parameters of Taylor Sandstone (Thomsen, 1986): $\alpha = 3.368$ km/s, $\beta = 1.829$ km/s, $\varepsilon = 0.110$, $\delta = -0.035$, i.e., $\eta > 0$ for this material.

We observe in Figure 1 that the dispersion relation becomes imaginary at the horizontal P-wave velocity, but turns real again for larger k_x (Amazonas et al., 2010). These larger wavenumbers correspond to a slower wave propagation, as we can see in Figure 2. Also shown in this Figure is the surface $a = 1$, which separates the domains for qP and qSV-wave propagation.

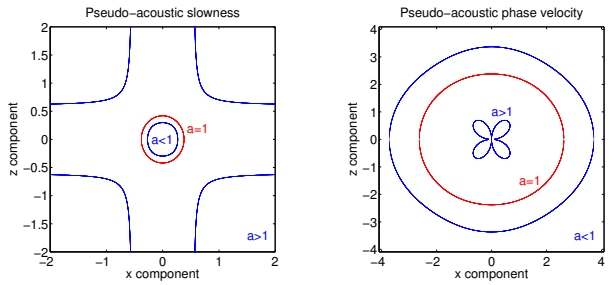

Figure 2: Slowness and phase-velocity surfaces for Taylor Sandstone. The domains for qP and qSV propagation are separated by the surface $a = 1$ (red line).

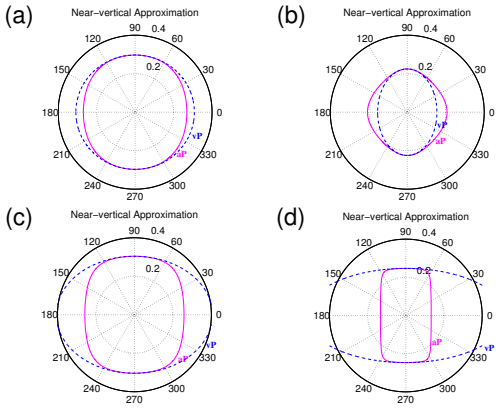

Figure 3: Pseudo-acoustic slowness surface (magenta line) and its near-vertical approximation (dashed blue line) for (a) Taylor Sandstone; (b) Mesaverde Laminated Siltstone; (c) dry Green River Shale; (d) Biotite Crystal.

qP relation for near-vertical propagation

Our first approximation for the pure qP dispersion relation is equation (31) for near-vertical propagation. Figure 3 shows this approximation for four different materials of Thomsen (1986) with very different anisotropies. These are Taylor Sandstone ($\alpha = 3.368$ km/s, $\beta = 1.829$ km/s, $\varepsilon = 0.110$, $\delta = -0.035$), Mesaverde Laminate Siltstone ($\alpha = 4.449$ km/s, $\beta = 2.585$ km/s, $\varepsilon = 0.091$, $\delta = 0.565$), dry Green River Shale ($\alpha = 3.292$ km/s; $\beta = 1.768$ km/s, $\varepsilon = 0.195$, $\delta = -0.220$), and Biotite Crystal ($\alpha = 4.054$ km/s, $\beta = 1.341$ km/s, $\varepsilon = 1.222$, $\delta = -0.388$). We see that in all cases the approximation correctly describes the slowness surface for propagation directions up to about 25-30°.

Small b approximation

Better approximation is achieved for all of these materials with the small b approximation of equation (34), previously derived by Klíe and Toro (2001). A comparison to the true pseudo-acoustic slowness surface for the four cited materials is shown in Figure 4. We see that for Taylor Sandstone (Figure 4a) and Mesaverde Laminated Siltstone (Figure 4b) the small b approximation is virtually indistinguishable from the pseudo-acoustic slowness surface. Even for the rather strongly anisotropic dry Green River Shale (Figure 4c), the differences in the diagonal directions are quite small. Only for the extremely anisotropic Biotite Crystal (Figure 4d), significant differences are visible.

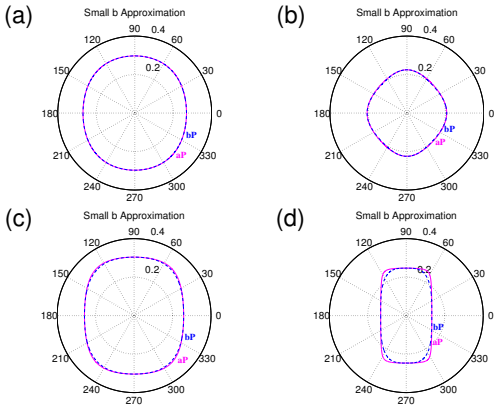

Figure 4: Pseudo-acoustic slowness surface (magenta line) and its small b approximation (dashed blue line) for (a) Taylor Sandstone; (b) Mesaverde Laminated Siltstone; (c) dry Green River Shale; (d) Biotite Crystal.

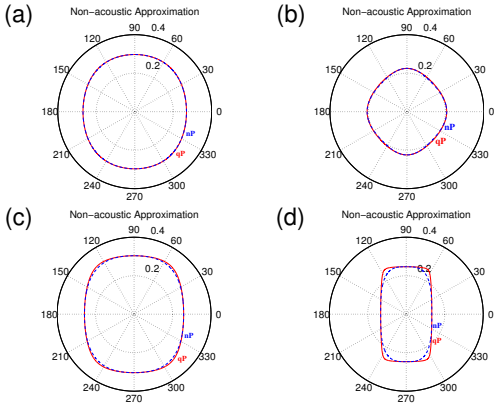

Figure 5: True qP slowness surface (red line) and its non-acoustic approximation (dashed blue line) for (a) Taylor Sandstone; (b) Mesaverde Laminated Siltstone; (c) dry Green River Shale; (d) Biotite Crystal.

Non-acoustic approximations

Next, we analyse the quality of the non-acoustic approximations of equations (37) and (40). Figure 5 compares the approximation of equation (37), previously derived by Pestana et al. (2012), to the true qP slowness surface. The quality of the approximation is practically identical to the one of equation (34) of Klíe and Toro (2001) with respect to the pseudo-acoustic slowness surface.

Figure 6 demonstrates the improved quality of the strong-anisotropy approximation. Even for the Biotite Crystal (Figure 6d), no deviation between the true and approximated slowness surfaces is visible. Here, we used the theoretical value of $q_1 = 1/2$ for the first Padé coefficient, but chose the second one q_2 to be represented in dependence on ε and δ according to the function $q_2 = 3.75 + 2\varepsilon - 3\delta/10$ instead of the conventional value $q_2 = 1/4$.

Figure 7 shows the relative error of the slowness as a function of the propagation angle for the chosen materials for the theoretical and optimized value of q_2. We see that the error is visibly reduced when using the latter.

Propagation snapshots

Encouraged by these very good approximations of the slowness surface, we implemented a low-rank scheme to simulate numerical wave propagation by means of

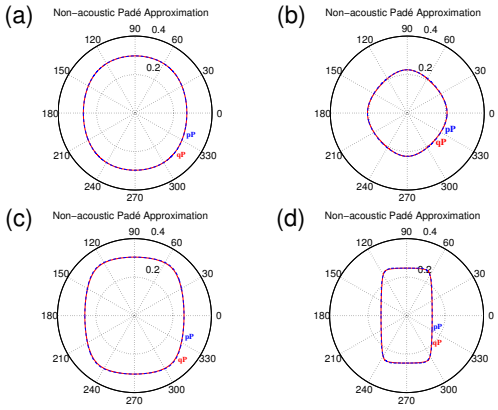

Figure 6: True qP slowness surface (red line) and its non-acoustic Padé approximation (dashed blue line) for (a) Taylor Sandstone; (b) Mesaverde Laminated Siltstone; (c) dry Green River Shale; (d) Biotite Crystal.

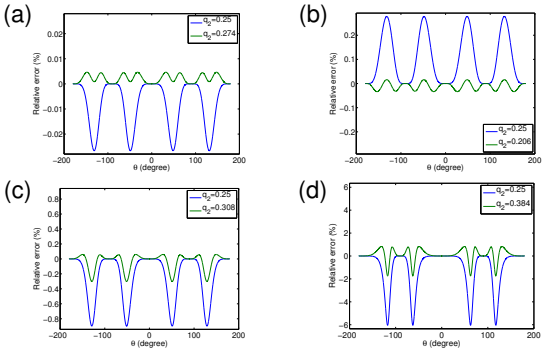

Figure 7: Error of non-acoustic slowness surface for theoretical (blue line) and optimized value of q_2 (green line) for (a) Taylor Sandstone; (b) Mesaverde Laminated Siltstone; (c) dry Green River Shale; (d) Biotite Crystal.

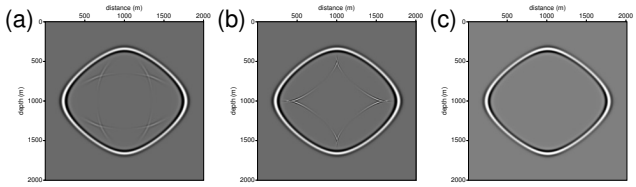

Figure 8: Snapshots of qP wave in a homogeneous dry Green River Shale. (a) Full tension wavefield. (b) Pseudo-acoustic wavefield. (c) Non-acoustic strong-anisotropy approximation.

these equations. Figure 8 compares the snapshots in a homogeneous dry Green River Shale and Figure 9 in Biotite Crystal. In both figures, part (a) shows the true wavefield with qP and qSV waves, part (b) shows the pseudo-acoustic wavefield with the approximate qP wave and an incorrect qSV wave, and part (c) shows the non-acoustic Padé approximation to the pure qP wave. We recognize that even for these media with very strong anisotropy, the non-acoustic Padé approximation provides a very good approximation of the qP wavefront, while eliminating the S mode entirely.

Inhomogeneous medium

Our final test simulated qP wave propagation in an inhomogeneous anisotropic TTI medium. The medium parameters are: Vertical constant gradient in α from 2.5 km/s at the top of the model to 4.5 m/s at the

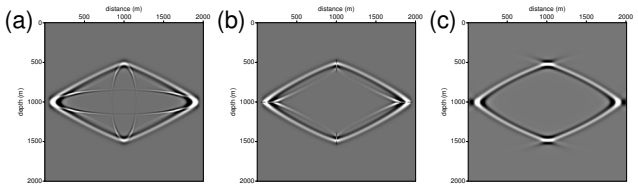

Figure 9: Snapshots of qP wave in a homogeneous Biotite Crystal. (a) Full tension wavefield. (b) Pseudo-acoustic wavefield. (c) Non-acoustic strong-anisotropy approximation.

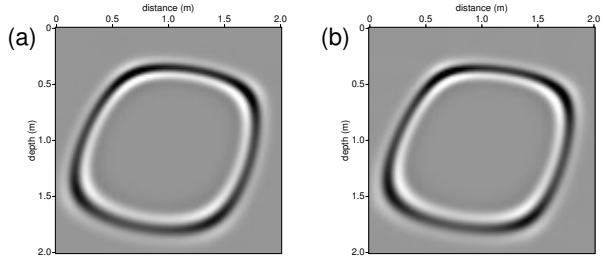

Figure 10: Snapshots of qP wave in an inhomogeneous anisotropic TTI model. (a) True qP wavefield. (b) Non-acoustic strong-anisotropy approximation.

bottom, homogeneous $\varepsilon = 0.195$ and $\delta = -0.220$ (taken from the dry Green River Shale), and symmetry axis tilted by an angle of 30° from the vertical. Figure 10 compares the result of low-rank approximate modeling of the exact qP dispersion relation (Figure 10a) with the result of approximate equation (40) (Figure 10b). Even for this rather strong anisotropy and velocity gradient, we observe almost perfect coincidence between the true and approximated wavefields.

Conclusions

We have studied elastic wave propagation in a VTI medium in order to better understand the coupling of qP and qSV wave propagation in the pseudo-acoustic approximation. We have found that the pseudo-acoustic qP dispersion relation of Alkhalifah (2000) is actually a coupled equation that describes both qP and a qSV waves. The equation can be uncoupled if the individual eikonal equations are considered. Since these equations contain square roots, they cannot be directly converted into differential approximations. Even their implementation by means of a low-rank approximation might be impaired in heterogeneous and strongly anisotropic media, as indicated by Wu and Alkhalifah (2014).

Therefore, we have discussed several approximations to the square root and found that some of them have already been derived in the literature by decoupling Alkhalifah's dispersion relation. A Padé approximation with slightly unconventional numbers for the Padé coefficients led to the best approximation. An implementation of a low-rank approximation to this equation demonstrated that is can provide high-accuracy wavefields even in strongly anisotropic inhomogeneous media. Using the new equation, we hope to explore in the near future its potential to provide an approximation that factors heterogeneity and anisotropy even in strongly anisotropic media in the fashion used by Liu et al. (2009) and Pestana et al. (2012) for weak anisotropy.

Acknowledgments

This work was kindly supported by the Brazilian government agencies CAPES, FINEP, and CNPq as well as Petrobras and the sponsors of the *Wave Inversion Technology (WIT) Consortium*.

References

Alkhalifah, T., 1998, Acoustic approximations for processing in transversely isotropic media: Geophysics, **63**, 623–631.

———, 2000, An acoustic wave equation for anisotropic media: Geophysics, **65**, 1239–1250.

———, 2003, An acoustic wave equation for orthorhombic anisotropy: Geophysics, **68**, 1169–1172.

Amazonas, D., R. Aleixo, J. Schleicher, and J. C. Costa, 2010, Anisotropic complex Padé hybrid finite-difference depth migration: Geophysics, **75**, S51–S59.

Bloot, R., J. Schleicher, and L. T. Santos, March, 2013, On the elastic wave equation in weakly anisotropic vti media: Geophysical Journal International, **192**, 1144–1155.

Červený, V., 1985, The application of ray tracing to the numerical modeling of seismic wavefields in complex structures, part A: Theory, *in* Seismic Shear Waves: Geophysical Press, volume **15** *of* Handbook of Geophysical Exploration, Section I: Seismic, 1–124.

Červený, V., 2001, Seismic ray theory: Cambridge University Press.

Du, X., R. Fletcher, and P. J. Fowler, 2008, A new pseudo-acoustic wave equation for VTI media: 70th EAGE Annual Conf. and Exhibition Extended Abstract, EAGE, H033.

Du, X., P. Fowler, and R. Fletcher, 2014, Recursive integral time-extrapolation methods for waves: A comparative review: Geophysics, **79**, T9–T26.

Fletcher, R., X. Du, and P. Fowler, 2009, Reverse time migration in tilted transversely isotropic (TTI) media: Geophysics, **74**, WCA179–WCA187.

Fowler, P., X. Du, and R. Fletcher, 2010, Coupled equations for reverse time migration in transversely isotropic media: Geophysics, **75**, S11–S22.

Grechka, V., L. Zhang, and J. Rector, 2004, Shear waves in acoustic anisotropic media: Geophysics, **69**, 576–582.

Klíe, H., and W. Toro, 2001, A new acoustic wave equation for modeling in anisotropic media: SEG Technical Program Expanded Abstracts 2001, 1171–1174.

Liu, G., S. Fomel, L. Jin, and X. Chen, 2009, Stacking seismic data using local correlation: Geophysics, **74**, V43–V48.

Pestana, R. C., B. Ursin, and P. L. Stoffa, 2012, Rapid expansion and pseudo spectral implementation for reverse time migration in VTI media: J. Geophys. Eng., **9**, 291–301.

Sergey Fomel, S., L. Ying, and X. Song, 2013, Seismic wave extrapolation using lowrank symbol approximation: Geophysical Prospecting, **61**, 526–536.

Song, X., and T. Alkhalifah, 2013, Modeling of pseudoacoustic P-waves in orthorhombic media with a low-rank approximation: Geophysics, **78**, C33–C40.

Thomsen, L., 1986, Weak elastic anisotropy: Geophysics, **51**, 1954–1966.

Wu, Z., and T. Alkhalifah, 2014, The optimized expansion based low-rank method for wavefield extrapolation: Geophysics, **79**, T51–T60.